International Journal of Mining and Geo-Engineering

IJMGE

IJMGE 52-1 (2018) 17-21

DOI: 10.22059/ijmge.2018.65679

Cumulative Fatigue Damage Under stepwise Tension-Compression Loading

Hadi Haghgouei [a, *], Hamid Hashemolhosseini [b], Alireza Baghbanan [a]

[a] *Department of Mining Engineering, Isfahan University of Technology, Isfahan, Iran*

[b] *Department of Civil Engineering, Isfahan University of Technology, Isfahan, Iran*

Article History:

Received: 24 November 2016,
Revised: 14 February 2017,
Accepted: 08 March 2018.

ABSTRACT

Rock structures are subjected to cyclic tension-compression loading due to a blasting, earthquake, traffic, and injection-production in an underground storage case. Therefore, studying the fatigue behavior of rock samples under this type of loading is required. In this study, the accumulated fatigue damage for a Green Onyx rock sample consisting only one mineral composition with two-step high-low sequences of loading levels was investigated under a completely reversed loading condition. New apparatus based on the R.R. Moore fatigue test machine was designed to assess this type of loading. A comparison was conducted between the predicted behavior of the Linear Damage Rule and the experimental data and a new damage model was proposed based on the experimental observation. The results showed a good agreement between the proposed damage model and the experimental data.

Keywords : *Completely Reversed Loading, Cumulative Damage, Fatigue of rocks, Linear Damage Rule, Stress-Life method*

1. Introduction

Fatigue is the progressive failure of material by the growth of cracks under cyclic loading [1]. Predicting fatigue damage for structures which are subjected to cyclic loading is a complicated phenomenon. Failure occurs in a material at the stress level less than its ultimate strength or even yield strength when cyclic loading is conducted. A large number of rock structures is subjected to cyclic and repetitive loading. Beside many research works about fatigue failure in metals, the study about this phenomenon in rocks is very limited. Many rock engineering projects such as tunnel walls, excavation roofs and ribs, bridge abutments, dam and road foundations as well as underground geo-reservoirs, such as compressed air energy storage systems, superconducting magnetic energy storage systems and underground storage of CO_2, oil and gas in their whole life are subjected to cyclic loading due to blasting, earthquake, traffic and injection-production cycles in underground storage cases [2-6]. One of the methods to study the fatigue behavior is the cumulative damage theory. In the literature, there are a few reported research works about the cumulative damage process during the fatigue test in the field of rock mechanics. In this case, Xiao et al. proposed an inverted S-shaped nonlinear fatigue damage cumulative model, which was derived based on the law of axial irreversible deformation development of rock [7]. Moreover, in order to validate the inverted S-shaped model and to find a relatively appropriate damage variable and describe the fatigue damage of rock, six common methods for definition of damage variable (Energy dissipation method, Elastic modulus method, Maximum strain method, Residual strain method, Ultrasonic wave velocity method, Acoustic emission cumulative counts method) were examined and the advantages and disadvantages of them were evaluated based on the experimental data of a Granitic sample under cyclic loading [8]. Chen et al. studied the influence of temperature on mechanical properties of Granite under the compression fatigue loading. They found that there is a linear relationship between the damage parameters and the fatigue life of Granite, based on the elastic modulus at different temperatures [9]. Liu and He employed two fatigue damage variables to investigate the fatigue damage evolution of sandstone samples subjected to axial compression fatigue loads under a confining stress state [10]. They also proposed a new damage variable that was derived based on the residual volumetric strain to study the dynamic damage evolution of sandstone samples [11]. The above-mentioned experimental studies on rocks estimated the rock fatigue only under the compressive loading mode. While rock structures, in reality, may be subjected to the tension-compression loading due to vibration via blasting, earthquake, traffic or injection-recovery process, which induce the tension-compression strain [12]. The fatigue damage theories indicate that the fatigue damage is strongly associated with crack initiation and propagation. In a compression loading condition, the fatigue cracks may grow due to the existence of residual tensile stress fields near stress concentrators [13], but the fatigue life of the compression loading is far longer than that of the tension loading [14]. In the high-cycle fatigue failure, the value of mean stresses has a great impact on fatigue behavior of structures. Normal mean stresses are responsible for the opening and closure of microcracks. Because of the tensile normal stresses accelerates the rate of crack propagation by the opening of microcracks and compressive normal stresses prevents the growth of cracks by closing them, the tensile normal stresses have negative and compressive normal stresses have positive effects in terms of fatigue strength [15]. Another shortcoming of aforementioned studies is the necessity of sophisticated equipment as well as applying a very high-stress level up to 95 percent of the ultimate compressive strength of the samples, which leads to a high level of damage before the cyclic loading is started. Also, the basic problem of cumulative damage theory is the prediction of remaining life of specimen subjected to variable loading [16], which is not noted in the above-mentioned literature. In the present research work, firstly, the applicability of Linear Damage Rule (LDR) was investigated for rock samples by a developed apparatus

* Corresponding author Tel: +989356880271, *E-mail address:* h.haghgouei@mi.iut.ac.ir (H. Haghgouei).

based on a rotating beam fatigue testing machine (R.R.Moore), which is commonly used for laboratory fatigue tests on metals. Then, based on experimental results, a new model was proposed to predict the fatigue life of Green Onyx samples, consisting only calcite mineral, under a completely reversed loading condition.

2. Study of fatigue behavior of materials using stress-life method

Stress-Life (S-N) test focuses on the nominal stress required to cause a failure in some number of cycles and is distinguished from other fatigue analyses by several features: [17],

- Cyclic stress is the main factor for fatigue failure
- The conditions for high-cycle fatigue are satisfied:
    - High number of cycles to fatigue failure ($N > 10^3$)
    - Small plastic deformation

S–N fatigue testing is generally conducted using completely reversed loading. The term "completely reversed loading" states that the loading is varying around a zero mean stress. Stress-life fatigue tests are usually carried out on several identically prepared specimens at different completely reversed stress amplitudes. The first test is performed at a stress level slightly smaller than the ultimate tensile strength of the material. The other tests are conducted with stress levels lower than that used in the first step. This process is continued, and the results are presented as a plot of stress (S) against the number of cycles to failure (N). A log scale is almost always used for the number of cycles (N). The definition of cycle numbers to reach a failure or the fatigue life (N), the mean stress (S_m) and the stress amplitude (S_a) are illustrated in Fig. 1.

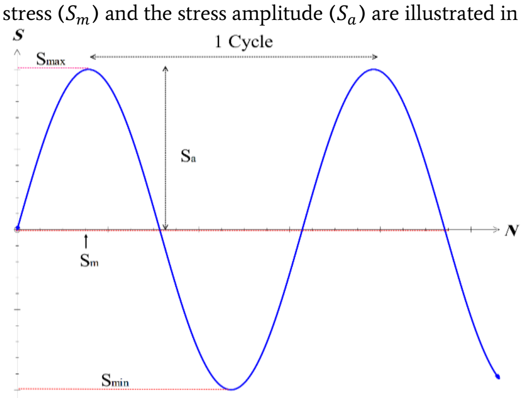

Fig. 1 Stress variation in a completely reversed loading.

3. Cumulative damage approach-linear damage rule

As mentioned before, one of the methods to assess the fatigue failure is the cumulative fatigue damage theory. Cumulative fatigue damage analysis plays a key role in life prediction of materials and structures that are subjected to field load histories [18]. The simplest and most used damage model to predict the fatigue life is the "linear damage rule", which is referred to the Miner's rule [19]. Miner proposed the LDR based on the Palmgren [20] and Langer's [21] research works. LDR states that if there are m different stress levels (multistep loading level) and the fatigue life (the number of cycles to failure) at the i[th] stress level is $N_{i,f}$, then the damage, D, can be expressed as follows,

$$D = \sum_{i=1}^{m} n_i / N_{i,f} \quad (1)$$

Where n_i is the number of cycles accumulated at i[th] stress level. Definition of LDR parameters is illustrated in Fig. 2.

According to LDR, the fatigue failure occurs when the damage value reaches unity. Commonly, LDR cannot properly estimate the fatigue life and often leads to non-conservative life predictions [15]. Thus, many attempts have been conducted to modify the Miner's rule.

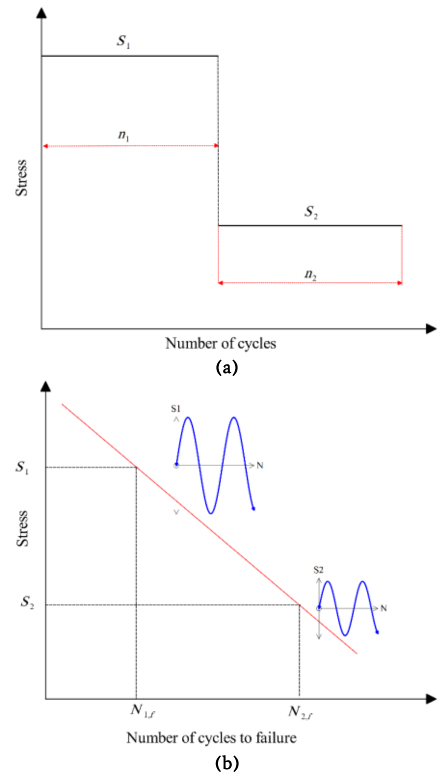

Fig. 2 Schematic presentation of **(a)** two-step high-low sequence of loading (variable amplitude loading) **(b)** S-N diagram (constant amplitude loading).

4. Testing equipment and sample preparations

There is no suggested method for determining the fatigue failure in rocks under the completely reversed loading condition. The most common types of fatigue machines are small bending fatigue ones. In general, these simple inexpensive systems allow laboratories to conduct extensive test programs with a reasonable equipment investment. In this work, a new apparatus based on the R.R.Moore test machine, which is commonly used for conducting the fatigue test in metal, is designed and a completely reversed loading was applied to investigate the fatigue behavior of Green Onyx samples.

4.1. Testing Device

In the newly developed machine, loading type is a completely reversed sinusoidal loading whose amplitude and frequency of loading are adjustable. The device is equipped with a sensor that automatically stops the testing operation upon the failures occur and records the number of cycles. The incorporated sensor and counter are capable of counting the number of performed cycles at 5000 rpm accurately. Fig. 3 explains the details of the test machine. By considering a rotating cantilever beam (Fig. 4), point A experiences a fully reversed sinusoidal loading. In this way, the stress level is calculated by the following equation,

$$S = FLy / I \quad (2)$$

where F is the applied load, L is the specimen length, I is the second moment of area about the neutral axis and y is the distance between point A and the neutral axis. When the specimen rotates, y changes depending on the frequency (ν) and time (t) as follows,

$$y = {}^{D}\!/_{2} \cos(2\pi \nu t) \quad (3)$$

where D is specimen diameter. According to equation (2) and (3) the final relation can be expressed as follows,

$$S = \left(\frac{32FL}{\pi d^3}\right) \cos(2\pi \nu t) \quad (4)$$

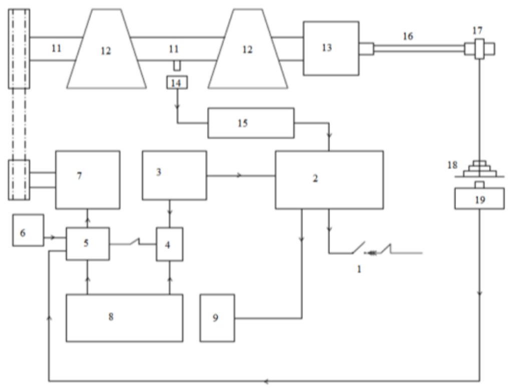

1. Switch
2. Switchboard
3. Power supply
4. AC to DC converter
5. Drive DC
6. Frequency regulator
7. Electric motor
8. Cooler panel
9. Electric fan
10. Pulley and belt
11. Axle
12. Bearing UCPA
13. Collet
14. Counter sensor
15. Autonics CT6S counter
16. Specimen
17. ball bearing
18. Loading set
19. Turn off Micro Switch

Fig. 3. Schematic flowchart of different pieces of the test machine.

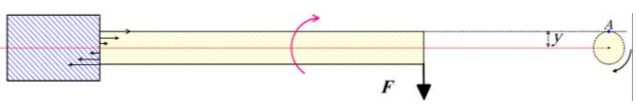

Fig. 4. Schematic presentation of the rotating beam under pure bending.

4.2. Specimen preparation

Green Onyx, a crystalline quarry stone and solely consisted of calcite mineral, was selected as the specimen. In the standard test specimens of R. R. Moore's rotating beam machine, the length/diameter ratio (*L/D* ratio) is about 11 [22]. A number of cylindrical specimens (core samples) with the length of 120mm and the diameter of 11mm were prepared by using a rotary drilling machine. This size of diameter has been previously reported for fatigue analysis in rocks [3]. Specimens were placed and fixed in two metal frames using epoxy resin. Since most of the fatigue cracks propagate from the surface of specimens, in order to reduce the effect of surface roughness in the geometric stress concentration, the surfaces of samples were polished carefully. The prepared specimen is shown in Fig. 5.

Fig. 5. Prepared specimen consisting the rock sample and steel frames.

In addition, the measured characteristic parameters of rock are tabulated in Table 1.

5. Fatigue test

Four levels of constant amplitude loading were performed based on the Ultimate Tensile Strength (stress level normalized by UTS) to assess the S-N diagram. The loading shape was sinusoidal in a completely reversed loading and the frequency during the test was kept at a constant value of 1.5 Hz. It should be noted that there is a considerable amount of scattering in constant amplitude fatigue test results. Consequently, a sufficient number of tests should be conducted to obtain a statistically meaningful result [17]. In this research work, three specimens were tested at each level of stress. Fatigue tests with several specimens at each stress level are called tests with replicate data [17]. S-N curve is more reliable when the percent of replication value is higher. The percent of replication (PR) is defined as follows,

$$PR = 100(1 - {}^{n_L}/_{n_s}) \tag{5}$$

In the above equation, n_L represents the number of stress levels and n_s is the sample size (number of specimen). The percent of replication for various purposes is listed below,

- 17–33 for preliminary and exploratory tests
- 33–50 for research and development tests
- 50–75 for design allowable data tests
- 75–88 for reliability data tests.

Table 1. Characteristics parameters of Green Onyx.

Rock type	Young's modulus (GPa)	Poisson ratio	Uniaxial compressive strength (MPa)	Ultimate tensile strength in bending (MPa)	Average grain diameter (mm)
Green Onyx	96	0.25	100.6	13.85	0.03

According to this equation, the PR for fatigue testing in this research work is 66 which is within the range for design stage. Therefore in this research work, the S-N curve is reliable enough. In the bending fatigue test, the maximum load is induced at the supported end of the sample. Therefore, the sample is expected to break from that location otherwise, failure in another place shall be considered as an error. Acceptable and unacceptable failure specimen are shown in Fig. 6. As can be seen in Fig. 5, all prepared samples consist of the rock sample and steel frame which are attached to rock. The suggested metallic specimens in the literature which have hourglass shaped test sections and difference in diameter can induce a residual stress into the samples. Therefore, stress concentration factor, K_t ,is usually approximated from the proposed charts in the text book[23]. Since the stiffnesses of steel and stone pieces are not the same, the graphs cannot be used for rock. Hence, Finite element analysis was performed at static state using Abaqus 6.1 software only for the purpose of determining the stress concentration ratio and verifying the location of the failure. The numerical simulation was conducted under maximum, minimum and average loading conditions. Fig. 7 shows stress distribution for Green onyx at maximum static bending load condition. The stress concentration factor was determined as 1.17 for Green Onyx samples. The S-N test results are presented in Table 2 and an S-N curve with loading frequency of 1.5 Hz is illustrated in Fig. 8.

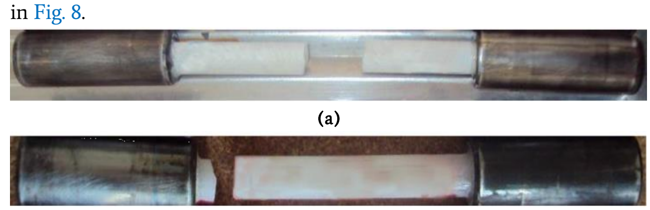

(a)

(b)

Fig. 6 (a) Broken specimen due to the previous flaw **(b)** true broken specimen after fatigue test.

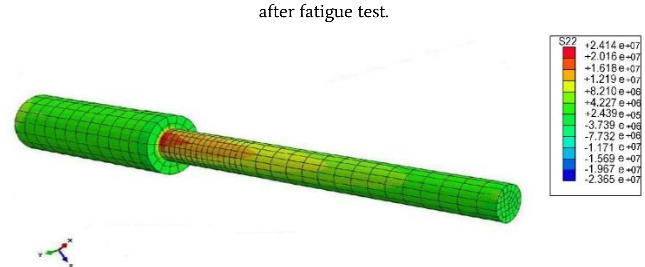

Fig. 7. Stress distributions for Green Onyx.

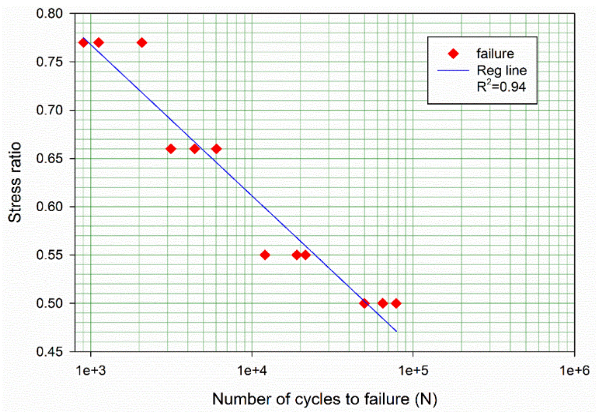

Fig. 8. S-N curve (Bending fatigue data) plotted on semi-log coordinates at 1.5 Hz frequency.

Table 2. Results of constant amplitude fatigue test for establishing the S-N diagram.

Specimen no.	Stress ratio	Fatigue life
1	0.77	902
2	0.77	2080
3	0.77	1121
4	0.66	4416
5	0.66	3143
6	0.66	6023
7	0.55	12049
8	0.55	18959
9	0.55	21476
10	0.5	64792
11	0.5	78518
12	0.5	49827

As can be seen, the number of cycles that a specimen withstands before the failure, is increased by decreasing the stress level. Also, the obtained results highlighted a linear trend in the variation of ultimate stress versus loading cycle number which resembles the presented results regarding the fatigue tests on other materials. In the high cyclic fatigue regime, the fatigue life is greater than 10^3 cycles and the test results confirmed this theory and number of cycles that a specimen withstands before the failure, is greater than 10^3 cycles. To study the cumulative damage during the fatigue test, the two-step high-low loading level was performed. In two-step high-low loading level, the initial high stress (s_1) level must be performed for n_1 cycles and then the test is continued through a low-stress level (s_2) until the failure occurs. The two stress levels are 9.2 and 8 MPa, which correspond to fatigue lives of 6630 and 16590 cycles, respectively, according to the S-N diagram. Schematic presentation of the two-step loading is presented in Fig. 9.

Four specimens were subjected to a two-step high-low loading test. The initial applied load cycles (n_1) at each test were selected randomly and the remaining cycle leading to failure (n_2) recorded during the test (experimental value presented in Table 3). The loading shape at each step was sinusoidal in a completely reversed loading and the frequency during the test was kept at a constant value of 1.5 Hz. It should be noted that a damage model is considered valid if the Relative Forecast Error (RFE) remains lower than 20% in absolute value [24]. The RFE, can be calculated as follows,

$$RFE = \frac{|Experimental\ Value - Theoretical\ Value|}{Experimental\ Value} \times 100 \qquad (6)$$

The initial cycles, theoretical (predicted by LDR) and experimental prediction of remaining cycles and the RFE are presented in Table 3.

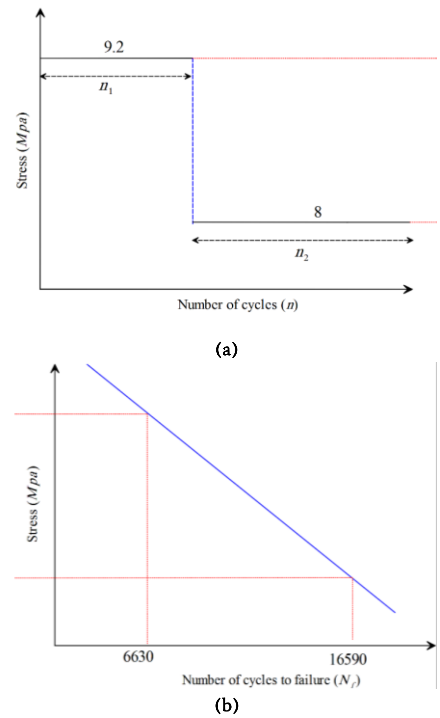

Fig. 9. Schematic presentation of (a) stepwise loading (b) S-N diagram at 1.5 Hz frequency.

Table 3. Initial cycles, Predicted value of remaining cycles and RFE by LDR.

Specimen no.	Initial cycles	Remaining cycles		RFE(%)
		experimental	theoretical	
T-S-1	1000	9290	14087	51.63
T-S-2	2000	6802	11585	70.31
T-S-3	2450	5807	10459	80.11
T-S-4	3250	3649	8457	131.76

From Table 3, it is clear that the linear damage rule cannot predict the fatigue behavior of rock, the LDR model is highly non-conservative, and the RFE values are above the acceptable threshold. According to the experimental results, the following damage equation for two-step loading is suggested,

$$D = \frac{n_1}{N_{1,f}} + \frac{n_2}{N_{2,f}} - 2\log\left(\frac{n_1}{N_{1,f}} + \frac{n_2}{N_{2,f}}\right) \qquad (7)$$

Equation (7) derived empirically to predict the remaining life (cycles) of Green Onyx specimen. The remaining cycles and RFE value calculated by equation 7 are presented in Table 4.

Table 4. Predicted value of remaining cycles and RFE by new damage rule.

Specimen no.	theoretical Remaining cycles	RFE(%)
T-S-1	9937	6.96
T-S-2	7448	9.49
T-S-3	6287	8.26
T-S-4	4296	17.73

As can be seen, the experimental data is in a very good agreement with the developed model and the RFE values are lower than acceptable threshold.

6. experimental verification of new damage model

In order to verify the proposed damage model, four two-step high-low sequence loadings were performed. The two stepwise stress levels are 9.2 and 6.9 MPa, which correspond to fatigue lives of 6630 and 50620 cycles, respectively, according to the S-N diagram. The results are presented in Table 5.

Table 5. Initial cycles and predicted value of remaining cycles and RFE by new damage rule.

Specimen no.	Initial cycles	Remaining cycles		Damage	RFE (%)
		experimental	theoretical		
T-S-5	500	33915	34117	1.000	0.59
T-S-6	1500	25310	26474	1.004	4.59
T-S-7	3000	15742	15034	0.997	4.49
T-S-8	3500	11136	11187	1.000	0.45

As can be seen, all the relatively forecasted errors are lower than 20% and the new damage model can accurately predict the fatigue behavior of the Green Onyx samples under the two-step loading.

Conclusion

Rock structures are usually exposed to variable amplitude cyclic loading and there is no suggested conventional standard method for determining the fatigue failure of rocks in the literature and all previous research works are related to the evaluation of fatigue behavior of rocks under compressional loading/unloading conditions. While rock structures, in reality, may be subjected to the tension-compression loading due to vibration via blasting, earthquake, traffic or injection-recovery process. In order to study the cumulative fatigue damage in rocks under the tension-compression condition, a new apparatus was designed based on the rotating beam fatigue testing machine (R.R.Moore) which is commonly used for laboratory fatigue test in metals and the applicability of linear damage rule introduced by Miner was investigated for the rock samples. A new damage model was proposed to predict the fatigue life of the Green Onyx samples under stepwise loading condition. The following conclusions associated with test results can be denoted,

- Although it is the first time that this method is used in rock mechanics field, the results showed a logical trend in Stress – Number of loading cycle diagram. The similarity between the mentioned test results and those obtained from the bending fatigue data in other materials indicate that the developed apparatus can be easily applied for investigating the fatigue behavior of rocks. The stress-life theory indicated that the fatigue life in high-cycle (elastic) region must be greater than 10^3 cycles and the test results satisfied this condition.
- Test results manifested that the linear damage rule cannot predict the fatigue behavior of rock and the LDR model is highly non-conservative and the RFE values are above the acceptable threshold.
- The new damage model is in a very good agreement with the experimental data and has a very good capacity to predict the final rupture.

Evaluation of the cumulative damage according to the new model is simple and all the parameters can be determined by means of the fitted S-N curve.

REFRENCES

[1] Shigley JE, Mischke CR, Budynas RG, Liu X, Gao Z. Mechanical engineering design. 9th ed. New York, USA: McGraw-Hill 2011.

[2] Bagde MN, Petroš V. Fatigue and dynamic energy behaviour of rock subjected to cyclical loading. *International Journal of Rock Mechanics and Mining Sciences*. 2009;46:200-9.

[3] Chen Y, Watanabe K, Kusuda H, Kusaka E, Mabuchi M. Crack growth in Westerly granite during a cyclic loading test. *Engineering Geology*. 2011;117:189-97.

[4] Liu J, Xie H, Hou Z, Yang C, Chen L. Damage evolution of rock salt under cyclic loading in unixial tests. *Acta Geotechnica*. 2014;9:153-60.

[5] Hou Z, Xie H, Were P. The special issue "Underground storage of CO2 and energy" in the framework of the 3rd Sino-German conference in May 2013. *Acta Geotechnica*. 2014;9:1-5.

[6] Chen J, Du C, Jiang D, Fan J, He Y. The mechanical properties of rock salt under cyclic loading-unloading experiments. *Geomechanics and Engineering*. 2016;10:325-34.

[7] Xiao J-Q, Ding D-X, Xu G, Jiang F-L. Inverted S-shaped model for nonlinear fatigue damage of rock. *International Journal of Rock Mechanics and Mining Sciences*. 2009;46:643-8.

[8] Xiao J-Q, Ding D-X, Jiang F-L, Xu G. Fatigue damage variable and evolution of rock subjected to cyclic loading. *International Journal of Rock Mechanics and Mining Sciences*. 2010;47:461-8.

[9] Chen Y-L, Ni J, Shao W, Azzam R. Experimental study on the influence of temperature on the mechanical properties of granite under uni-axial compression and fatigue loading. *International Journal of Rock Mechanics and Mining Sciences*. 2012;56:62-6.

[10] Liu E, He S. Effects of cyclic dynamic loading on the mechanical properties of intact rock samples under confining pressure conditions. *Engineering Geology*. 2012;125:81-91.

[11] Liu E, Huang R, He S. Effects of frequency on the dynamic properties of intact rock samples subjected to cyclic loading under confining pressure conditions. *Rock mechanics and rock engineering*. 2012;45:89-102.

[12] Chen X, Zhang Q, Li S, Liu D. Geo-mechanical Model Testing for Stability of Underground Gas Storage in Halite During the Operational Period. *Rock Mechanics and Rock Engineering*. 2016:1-15.

[13] Fleck N, Shin C, Smith RA. Fatigue crack growth under compressive loading. *Engineering fracture mechanics*. 1985;21:173-85.

[14] Qiao D, Wang G, Jiang W, Yokoyama Y, Liaw PK, Choo H. Compression-Compression Fatigue and Fracture Behaviors of Zr_{50} $Al_{10}Cu_{37}Pd_3$ Bulk-Metallic Glass. *Materials transactions*. 2007;48:1828.

[15] Lee Y-L. Fatigue testing and analysis : theory and practice. USA: Butterworth-Heinemann; 2005.

[16] Ben-Amoz M. A cumulative damage theory for fatigue life prediction. *Engineering Fracture Mechanics*. 1990;37:341-7.

[17] Lee Y-L, Jwo P, Richard BH, Mark EB. Fatigue testing and analysis: theory and practice: Butterworth-Heinemann; 2005.

[18] Fatemi A, Yang L. Cumulative fatigue damage and life prediction theories: a survey of the state of the art for homogeneous materials. *International journal of fatigue*. 1998;20:9-34.

[19] Miner MA. Cumulative damage in fatigue. *Journal of applied mechanics*. 1945;12:159-64.

[20] Palmgren A. Die lebensdauer von kugellagern. *Zeitschrift des Vereins Deutscher Ingenieure*. 1924;68:339-41.

[21] Langer B. Fatigue failure from stress cycles of varying amplitude. *Journal of Applied Mechanics*. 1937;59:A160-A2.

[22] Budynas RG, Nisbett J. Shigley's mechanical engineering design. 8th ed: McGraw-Hill, New York; 2008. p. 1059.

[23] Richard Budynas, Nisbett K. Shigley's Mechanical Engineering Design. 10th ed: McGraw-Hill 2011.

[24] Ghammouri M, Abbadi M, Mendez J, Belouettar S, Zenasni M. An approach in plastic strain-controlled cumulative fatigue damage. *International Journal of Fatigue*. 2011;33:265-72.